Electronic Supplementary File

Multidimensional $Na_4VMn_{0.9}Cu_{0.1}(PO_4)_3$/C Cotton-candy Cathode Materials for High Energy Na-ion Batteries†

*Vaiyapuri Soundharrajan,[a] Muhammad H. Alfaruqi,[a,b] Seulgi Lee,[a] Balaji Sambandam,[a] Sungjin Kim,[a] Seokhun Kim,[a] Vinod Mathew,[a] Duong Tung Pham,[c] Jang-Yeon Hwang,[a] Yang-Kook Sun,[d] and Jaekook Kim[a]**

[a]Department of Materials Science and Engineering, Chonnam National University,
300Yongbong-dong, Bukgu, Gwangju 500-757, South Korea; Fax: +82-62-530-1699; Tel: +82-62-530-1703

[b]Departemen Teknik Metalurgi, Universitas Teknologi Sumbawa, Jl. Raya Olat Maras, Sumbawa, Nusa Tenggara Barat, 84371, Indonesia

[c]Institute for Electrochemical Energy Storage, Helmholtz-Zentrum Berlin für Materialien und Energie, Hahn-Meitner-Platz 1, 14109 Berlin, German

[d]*Department of Energy Engineering, Hanyang University, Seoul 133-791, South Korea.*

*E-mail: jaekook@chonnam.ac.kr

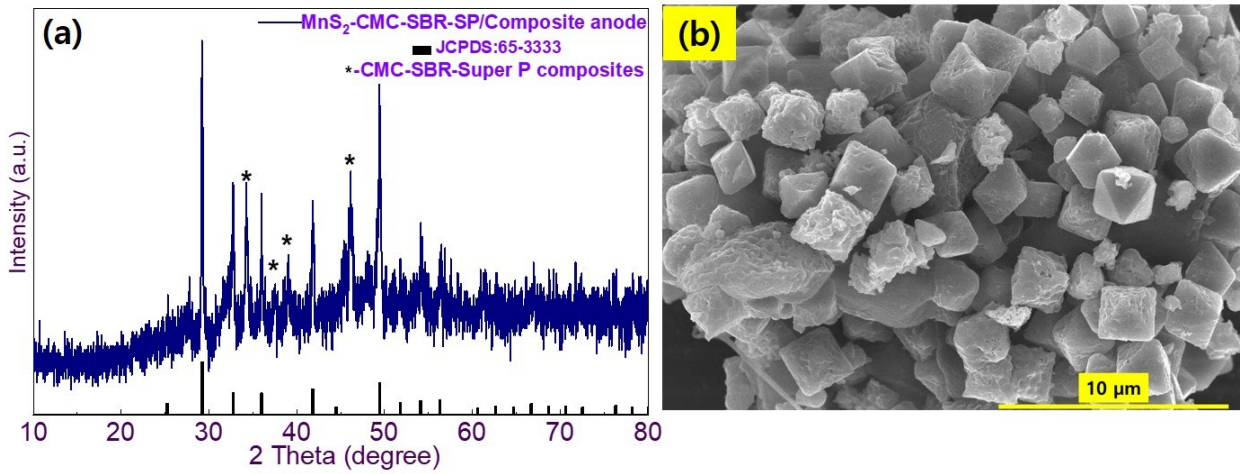

Fig. S1. (a) PXRD pattern and (b) FE-SEM image of the MnS_2 anode.

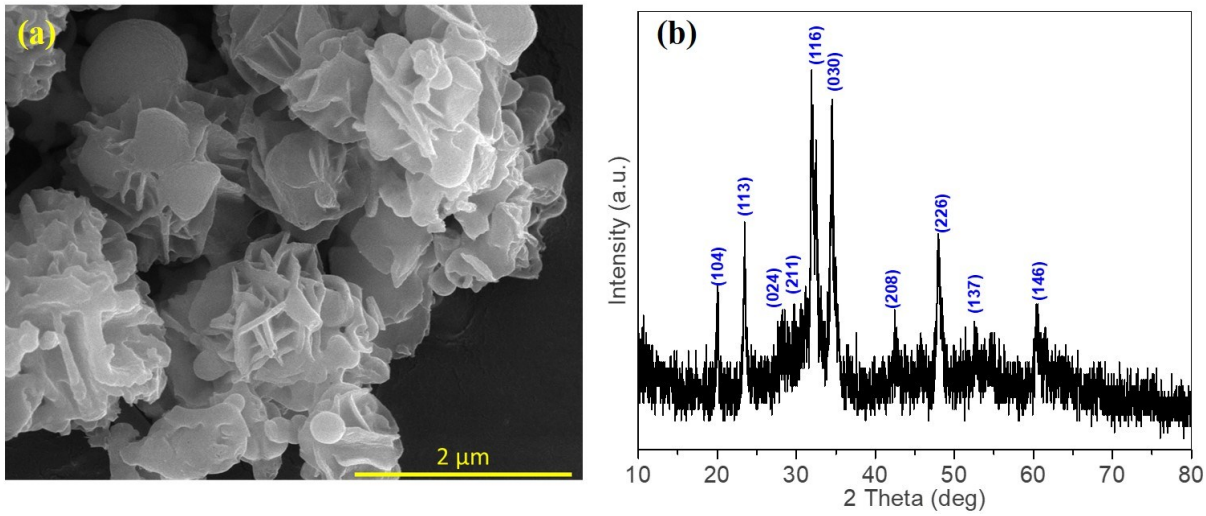

Fig. S2. (a) SEM image of the combustion deposits, (b) PXRD pattern of the combustion deposits.

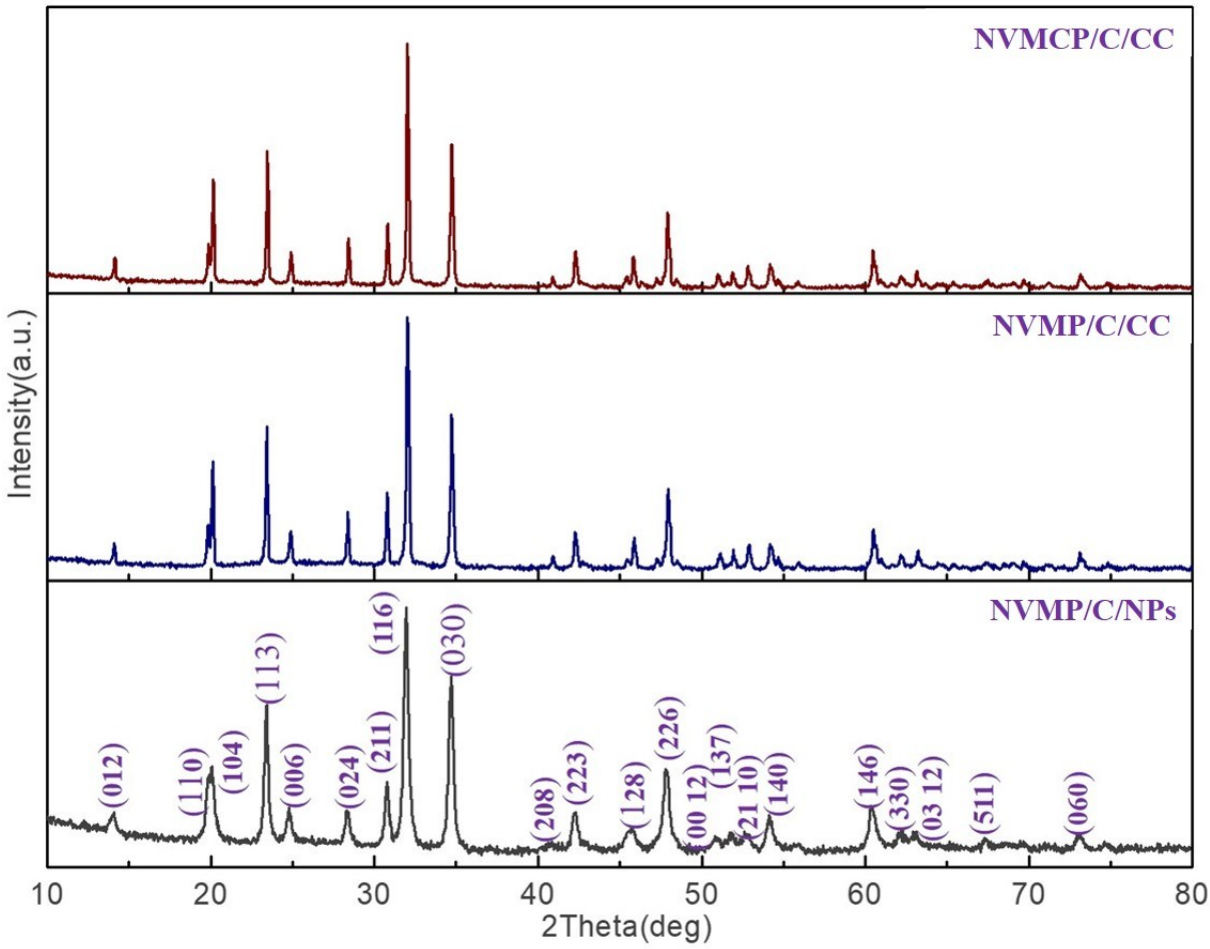

Fig. S3. Comparison of XRD pattern for NVMP/C/NPs, NVMP/C/CC, and NVMCP/C/CC.

Element	Wyckoff Positions			SOF	B_{iso}
	x	y	z		
Na	0	0	0	1.0	1.0
Na	0.6425	0	0.25	1.0	1.0
V	0	0	0.14901	0.5	1.0
Mn	0	0	0.14901	0.5	1.0
P	0.298	0	0.25	1.0	1.0
O	0.0136	0.209	0.1932	1.0	1.0
O	0.1863	0.1721	0.0852	1.0	1.0
R_{wp} = 4.009, R_p = 2.73, R_{exp} = 3.42, GoF = 1.36					
a = b = 8.9649 Å, c = 21.47864 Å; α = β =90˚, γ = 120˚					

Table S1 Crystallographic data of the $Na_4VMn(PO_4)_3$ powder obtained from Rietveld refinement.

Element	Wyckoff Positions			SOF	B_{iso}
	x	y	z		
Na	0	0	0	1.0	1.0
Na	0.6425	0	0.25	1.0	1.0
V	0	0	0.14901	0.5	1.0
Mn	0	0	0.14901	0.45	1.0
Cu	0	0	0.14901	0.05	1.0
P	0.298	0	0.25	1.0	1.0
O	0.0136	0.209	0.1932	1.0	1.0
O	0.1863	0.1721	0.0852	1.0	1.0
R_{wp} = 4.009, R_p = 2.73, R_{exp} = 3.42, GoF = 1.36					
a = b = 8.96072 Å, c = 21.48843 Å; α = β =90˚, γ = 120˚					

Table S2 Crystallographic data of the $Na_4VMn_{0.9}Cu_{0.1}(PO_4)_3$ powder obtained from Rietveld refinement.

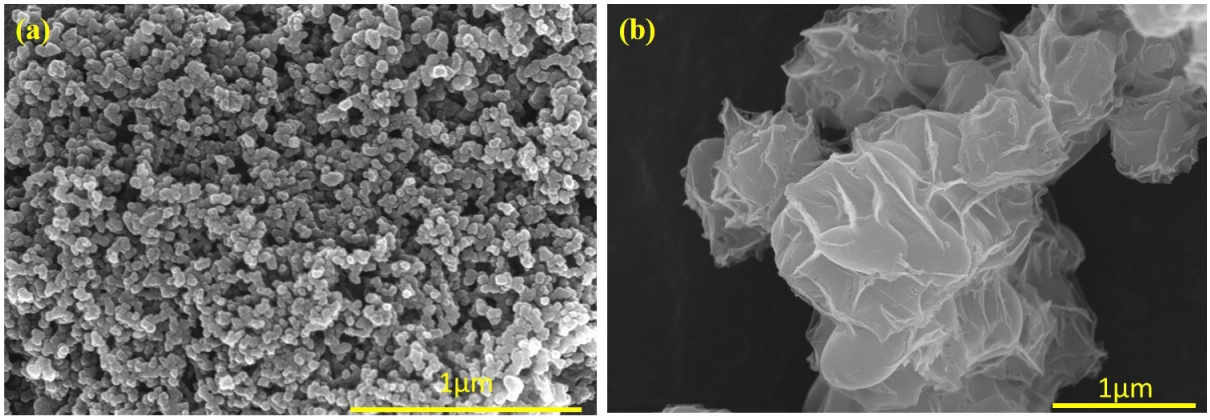

Fig. S4. (a) SEM image of the NVMP/C/NPs (b) SEM image of the NVMP/C/CC.

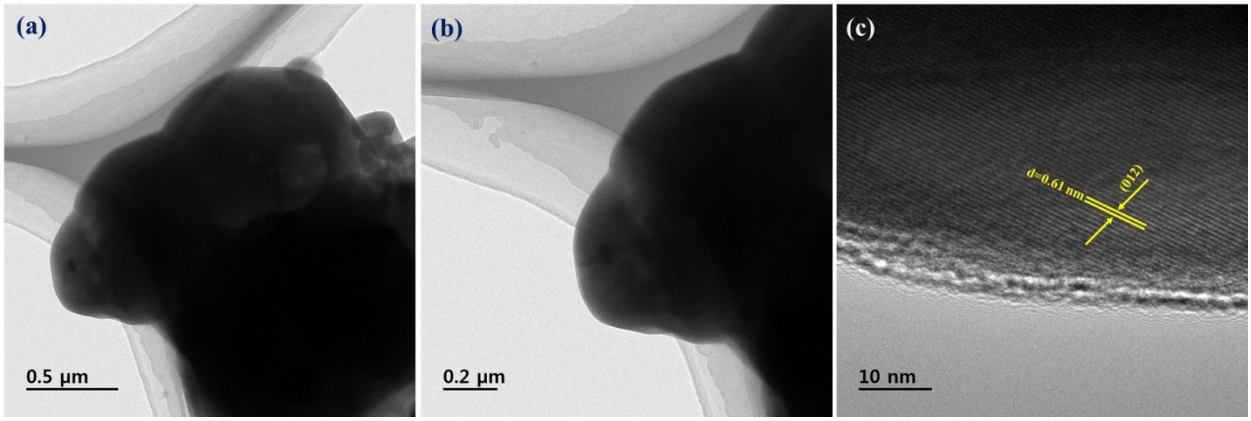

Fig. S5. Additional TEM image of the $Na_4VMn_{0.9}Cu_{0.10}(PO_4)_3$ cotton candy (a) and (b) low-resolution images, and (c) local-magnification image.

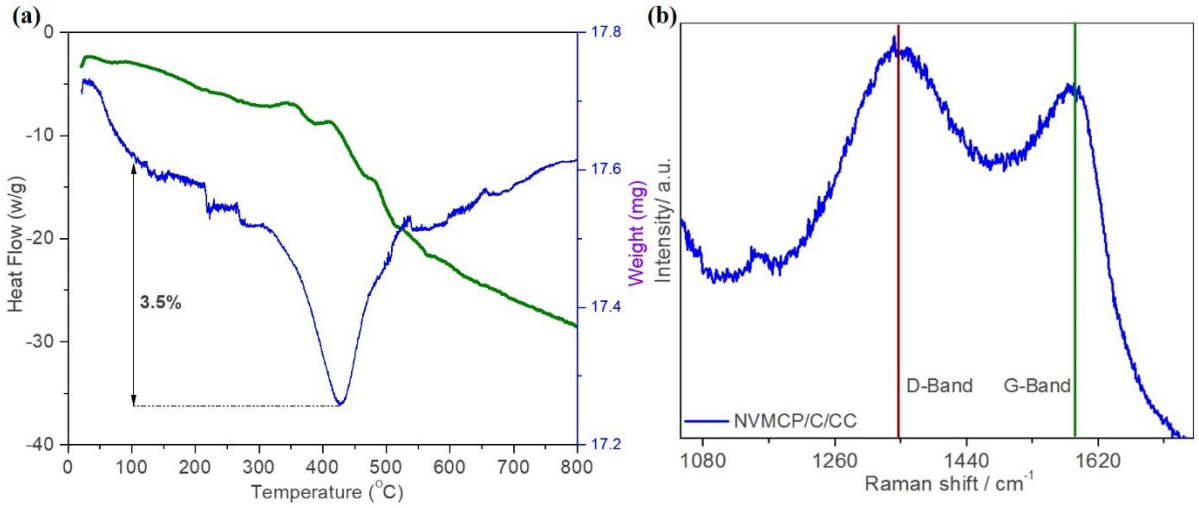

Fig. S6. (a) Thermogravimetric and (b) Raman spectra of the NVMCP/C/CC.

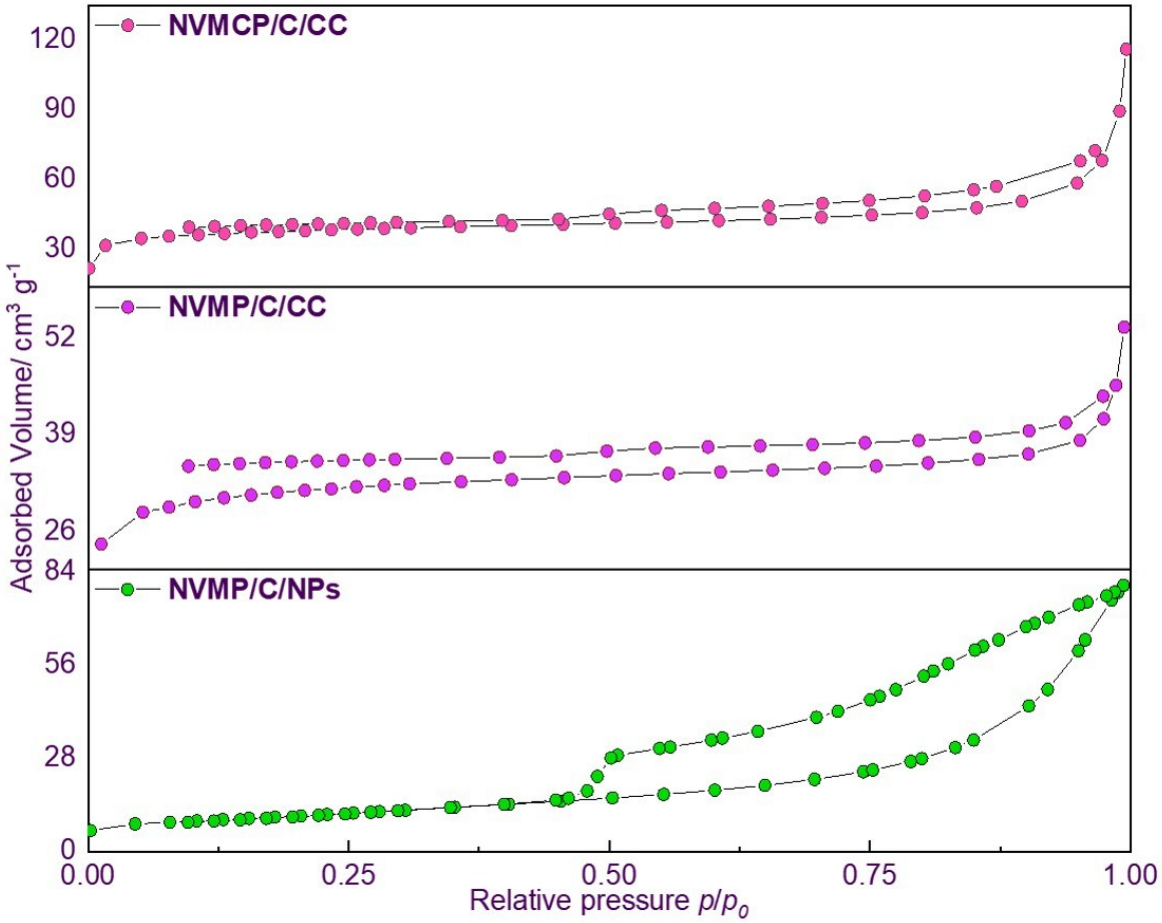

Fig. S7. Nitrogen adsorption/desorption isotherms of the NVMP/C/NPs, NVMP/C/CC, and NVMCP/C/CC.

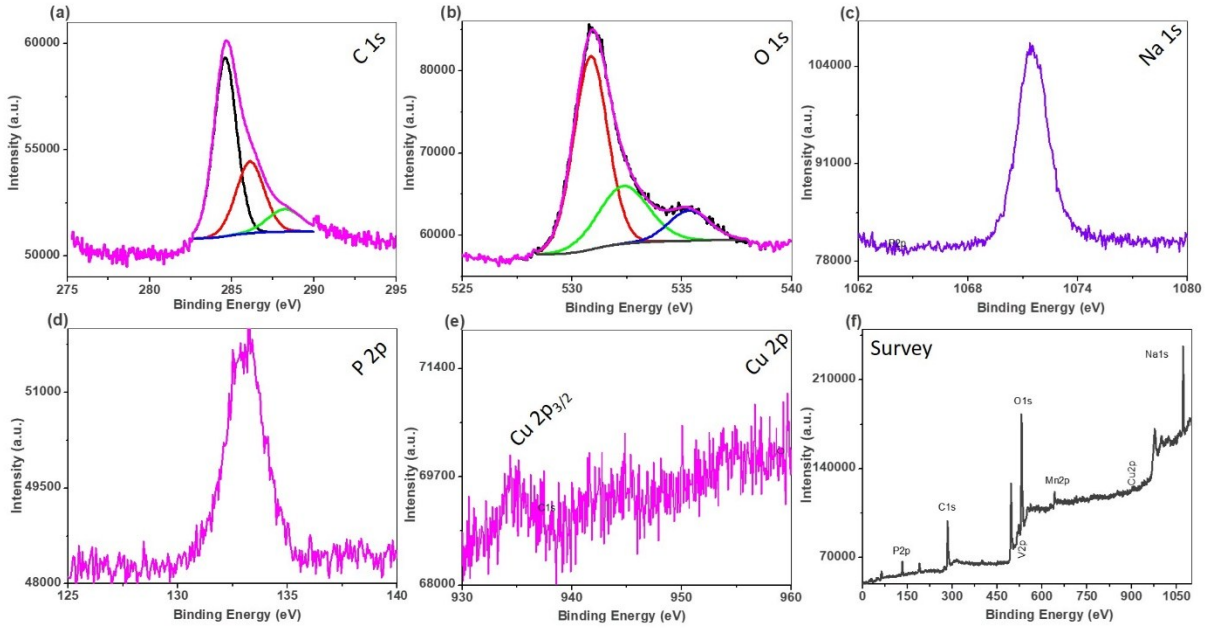

Fig. S8. XPS profile for NVMCP/C/CC (a) C 1s; (b) O1s; (c) Na 1s; (d) P 2p; (e) Cu 2p and (f) survey spectrum.

Element	Wavelength (nm)	Concentration (wt %)
Na	589.592	12.9
V	290.88	8.2
Cu	327.393	1
Mn	257.61	7.92
P	213.617	12.2

Table S3. ICP-OES analysis of $Na_4VMn_{0.9}Cu_{0.10}(PO_4)_3$ powder.

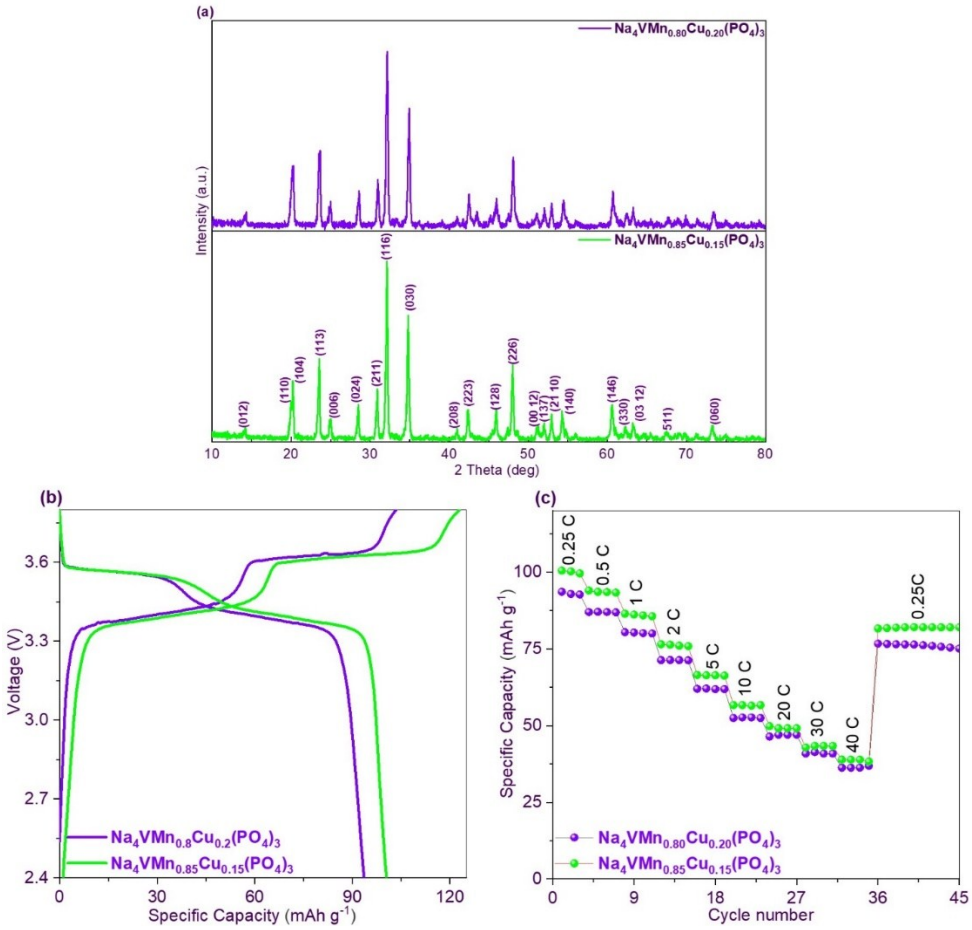

Fig. S9. (a) PXRD profile of $Na_4VMn_{0.85}Cu_{0.15}(PO_4)_3$ and $Na_4VMn_{0.8}Cu_{0.20}(PO_4)_3$ electrodes, (b) Charge/discharge profile of $Na_4VMn_{0.85}Cu_{0.15}(PO_4)_3$ and $Na_4VMn_{0.8}Cu_{0.20}(PO_4)_3$ electrodes at 0.25 C rate, (c) rate profile plot for $Na_4VMn_{0.85}Cu_{0.15}(PO_4)_3$ and $Na_4VMn_{0.8}Cu_{0.20}(PO_4)_3$ electrodes at various current rates.

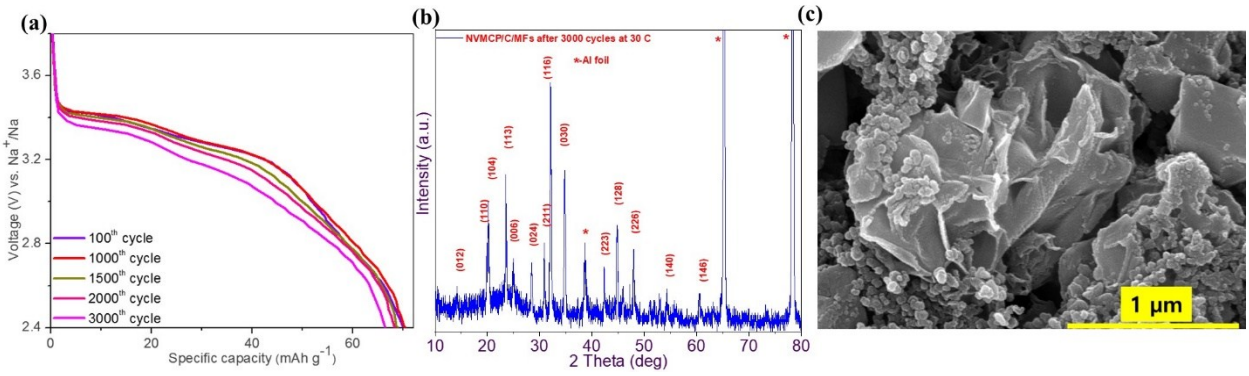

Fig. S10. (a) Discharge profile for NVMCP/C/CC cathode at 30 C rate, (b) *ex situ* XRD profile, and (c) *ex situ* SEM image for the NVMCP/C/CC cathode at 30 C rate after 3000 cycles.

Composite	Preparation method	Morphology	Rate capability	Cycling stability
$Na_4MnV(PO_4)_3/C$ [1]	Sol-gel	Worm-like	90 mAh g^{-1} at 10 C	89% at 1C (1000 cycles)
$Na_4MnV(PO_4)_3/C/GA$ [2]	Sol-gel	Nano-grains	88.1 mAh g^{-1} at 10 C 77.3 mAh g^{-1} at 20 C	68.8 % at 20 C (4000 cycles)
$Na_4MnV(PO_4)_3/C/rGO$ [3]	Sol-gel	Inter-connected nanoparticles	65 mAh g^{-1} at 20 C	91 % at 0.1 C (60 cycles)
$Na_4MnV(PO_4)_3/C/CNT$ [4]	Wet-chemical	Inter-connected nanoparticles	71 mAh g^{-1} at 80 C	84 % at 20 C (2000 cycles)
$Na_4MnV(PO_4)_3/rGO/AC$ [5]	Spray-drying	Microspherical	45.1 mAh g^{-1} at 9 C	78 % at 9 C (500 cycles)
$Na_4VMn_{0.9}Cu_{0.1}(PO_4)_3/C/CC$ (This work)	Pyro-synthesis	Cotton-candy	68 mAh g^{-1} at 40 C	86 % at 30 C (3000 cycles)

Table.S4. Comparison of electrochemical performance between $Na_4VMn_{0.9}Cu_{0.1}(PO_4)_3/C/CC$ and other reports .

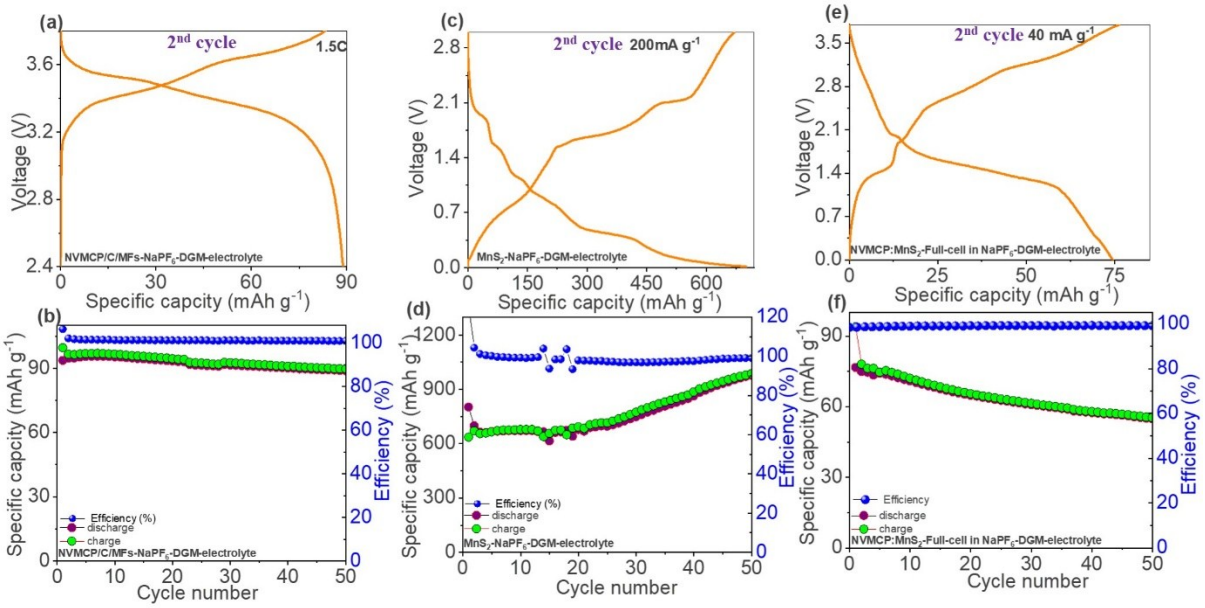

Fig. S11. a) Galvanostatic charge/discharge profile and (b) cyclability plot of the $Na_4VMn0_{.9}Cu_{0.1}(PO_4)_3$ cathode at 1.5 C in 1.0 M $NaPF_6$ in DGM electrolyte, (c) Galvanostatic charge/discharge profile and (d) cyclability plot of the MnS_2 anode at 200 mA g^{-1} in 1.0 M $NaPF_6$ in DGM electrolyte. Electrochemical performance of NVMCP/C/CC/MnS_2 full-cell in 1.0 M $NaPF_6$ in DGM electrolyte; (e) Galvanostatic charge/discharge profile and (f) cyclability plot in the potential range of 0-3.6 V at 40 mA g^{-1}.

References:

1. W. Zhou, L. Xue, X. Lü, H. Gao, Y. Li, S. Xin, G. Fu, Z. Cui, Y. Zhu and J. B. Goodenough, *Nano Lett.*, 2016, **16**, 7836–7841.
2. H. Li, T. Jin, X. Chen, Y. Lai, Z. Zhang, W. Bao and L. Jiao, *Adv. Energy Mater.*, 2018, **8**, 1801418
3. P. Ramesh Kumar, A. Kheireddine, U. Nisar, R. A. Shakoor, R. Essehli, R. Amin and I. Belharouak, *J. Power Sources*, 2019, **429**, 149–155.
4. W. Zhang, Z. Zhang, H. Li, D. Wang, T. Wang, X. Sun, J. Zheng and Y. Lai, *ACS Appl. Mater. Interfaces*, 2019, **11**, 35746–35754.
5. C. Cai, P. Hu, T. Zhu, C. Chen, G. Hu, Z. Liu, Y. Tian, Q. Chen, L. Zhou and L. Mai, *J. Phys. Energy* 2020, **2**, 025003.